Korean J. Chem. Eng., **29**(8), 1057-1062 (2012)
DOI: 10.1007/s11814-011-0292-1

The influence of activated carbon support on nitrate reduction by Fe(0) nanoparticles

Misun Cho and Samyoung Ahn†

Department of Environmental Education, Sunchon National University, 413, Jungang-ro, Sunchon, Jeonnam 540-742, Korea
(*Received 7 August 2011 • accepted 19 November 2011*)

Abstract–Activated Carbon supported Fe(0) nanoparticles (AC-Fe(0)) were applied to the reductive removal of nitrate to investigate the effects of AC support on the reactivity of Fe(0) nanoparticle. XRD, SEM and EDS, XPS analyses on AC-Fe(0) revealed that AC-Fe(0) is more susceptible to oxidation compared to the unsupported Fe(0) nanoparticles, and that the extent of oxidation of the AC-Fe(0) particles will vary depending on the ratios of AC to Fe(0). Nitrate reduction rate of AC-Fe(0) was much slower than that of unsupported Fe(0) nanoparticles. AC-Fe(0) (0.5 : 1) particles reduced the nitrate to ca. 40% of the initial concentration, and AC-Fe(0) (5 : 1) particles performed poorly with only 10% removal of the nitrate. Besides the deactivation of AC-Fe(0) due to corrosion of Fe(0), the mass transport limitation caused by the thick layering of Fe(0) on porous AC seemed to be another negative factor for the decreased reactivity of AC-Fe(0).

Key words: Supported Fe(0), Fe(0) Nanoparticles, Activated Carbon, Nitrate Reduction, SEM-EDS, XPS

INTRODUCTION

Immobilization of nanoparticles to larger support particles seems to be an attractive strategy used to overcome aggregation and clumping of the nanoparticles and to improve their separation and hydraulic conductivity. In addition, the dispersion of active metals in nanoscale on a porous support material with a large surface area is expected to provide a large number of active sites and to increase the reactivity of nanoparticles. This idea is commonly practiced in reactions that involve heterogeneous catalysis [1,2].

In previous research [3], we found that Fe(0) nanoparticles supported on activated carbon, polyethylene, and silica show a significantly reduced reactivity for nitrate reduction. The supports tested showed a negative influence, with the nitrate reduction rate decreasing in the order of unsupported Fe(0)>activated carbon supported Fe(0)>polyethylene supported Fe(0)≥silica supported Fe(0). This result was unexpected, as the large surface area of support and the fine distribution on the support surface were expected to be beneficial to the reaction activity of catalyst metals.

There has been much work on applications of zerovalent iron nanoparticles on the treatment of pollutants, but studies on supported zerovalent iron nanoparticles are rare. Mallouk et al. reported on reductive remediation of Cr(VI) and Pb(II) using nanoscale Fe(0) supported on the polymer resin [4,5]. In their study, the resin supported Fe(0) showed a similar reactivity as to the unsupported Fe(0). Another report on the application of the supported Fe(0) dealt with the separation and reduction of pertechnetate anions (TcO_4^-) from simulated nuclear waste streams [6]. In this report, the TcO_4^- removal efficiency of the silica supported Fe(0) was similar to that of unsupported Fe(0). Another report on the chitosan and silica supported Fe(0) for the dechlorination of 1,2,4-trichlorobenzene can be added to a simple list of publications about the supported Fe(0) [7]. However, they provided only the results with supported Fe(0), leaving out any comparative data of unsupported Fe(0). Cellulose acetate supported Fe(0) nanoparticles reduced trichloroethylene (TCE) in the same order as unsupported Fe(0) nanoparticles [8].

All of these studies conducted on supported Fe(0), so far, have failed to yield enhanced reactivity and there has not been any clear explanation for these results. The question of why supported Fe(0) did not show an enhanced performance in their application and how the results are related to the modified physico-chemical characteristics of supported Fe(0) should be addressed. These unpredicted results from former researches and our previous experience prompted us to investigate the physicochemical properties and reactivity of supported Fe(0) on the treatment of pollutants in greater detail.

We did research on nitrate reduction with activated carbon supported iron nanoparticles (AC-Fe(0)). Nitrate (NO_3^-) is the world's most widespread groundwater and drinking water contaminant [9], mainly resulting from fertilizers, animal manure and atmospheric deposition from nitrogen oxide emission. Consumption of NO_3^- can lead to methemeglobmenia in infants, and with long-term exposure is a possible cancer risk [10,11]. For these reasons, there is a major effort to keep the nitrate concentration in drinking water below the maximum containment level of 10 mg/L NO_3^- N (44 mg/L as NO_3^-; USA and Korea) [12] and 11.3 mg/L NO_3^- N (50 mg/L as NO_3^-; European Community) [13].

AC was selected for study, because no studies exploring the effects of AC as a support for Fe(0) nanoparticles had been reported. Furthermore, AC has been widely used as an adsorbent of pollutants and as support for active metals in chemical treatments [14]. AC is not expensive and is available in various forms and size, and most importantly, environmentally benign.

EXPERIMENTAL

1. Chemicals

$FeSO_4 \cdot 7H_2O$ (>99%) was obtained from Kanto Chemical Co.

†To whom correspondence should be addressed.
E-mail: sahn@sunchon.ac.kr

(Japan), and KBH_4 (98%) was obtained from Aldrich. Activated Carbon was purchased from Aldrich (Darco. 12-20 mesh) and used after washing with deionized water. KNO_3 was purchased from Junsei Chemicals. All aqueous solutions were made in water purified with a Milli-Q system (18 MΩ/cm). All procedures for syntheses and handling during this experiment were carried out under an atmosphere of N_2 (99.9%), using standard glovebox techniques. All solvents were degassed and saturated with N_2 before use.

2. Preparation of AC-Fe(0) Particles

Activated carbon and $FeSO_4 \cdot 7H_2O$ were deoxygenated by a vacuum pump before adding KBH_4 and then filled with N_2. KBH_4 solution was added to a flask containing a given amount of activated carbon and $FeSO_4 \cdot 7H_2O$ at room temperature under stirring [4,15]. The solution was stirred until gas evolution ceased (ca. 1 h). AC-Fe(0) particles that formed eventually settled, and the supernatant was decanted with a double-tipped needle under N_2 atmosphere. Then the solid was washed with degassed and deionized water several times and finally with degassed acetone. The degassed acetone was prepared by bubbling N_2 through acetone under ice bath to prevent acetone from evaporating. The resulting gray-black solid was vacuum-dried.

3. Batch Experiments

For a batch experiment, typically, a given amount of AC-Fe(0) was charged into a three neck flask containing 1 L of 100 ppm nitrate solution under stirring. The nitrate solution was deoxygenated by N_2 bubbling for 2 h before adding AC-Fe(0). Periodically, 10 mL samples were withdrawn under N_2 stream and filtered through a 0.45 μm membrane filter (Advantec MFS).

Concentrations of nitrate were determined by ion chromatography (Dionex 120) consisting of GP 50 pump CD 25 conductivity detector, AS40 automated sampler and Dionex IonPac AS14 (4× 250 mm) analytical column. Samples drawn for the determination of ammonia were treated with a few drops of dilute HCl to trap ammonia as ammonium ion, which were then analyzed by UV spectrophotometer (Shimadzu 1600) using the Indophenol method of standard method [16].

A control experiment using a similar experimental setup but without Fe(0) was conducted to determine to what extent the nitrate would be adsorbed to AC support.

4. Analyses

BET surface areas were obtained at liquid nitrogen temperature, using a Surface Area Analyzer (ASAP-2010, Micromeritics) at Korea Basic Science Institute (Jeonju Center). Prior to the measurement, all samples were degassed under vacuum at 300 °C for 2 h. The specific surface areas were determined from a linear part of the BET plot.

Elemental analyses were performed at Korea Basic Science Institute (Seoul Center) with ICP-AES (Jobin Yvon, 138 Ultrace).

XRD were measured at Korea Basic Science Institute (Sunchon Center) with X'Pert Pro (PANalytical, Netherland) equipped with a graphite monochromator (Cu Kα radiation, λ=1.54056 Å). The analysis was carried out at 40 kV and 30 mA. The scan speed was set at 2θ of 5.4°/min, and the range was set from 10° to 90°.

Surface morphologies of nanoparticles were examined at Korea Basic Science Institute (Sunchon Center) by a FE-SEM (Hitachi S-4800). SEM combined with energy-dispersive X-ray spectrometry (EDS) was performed on a Bruker (X-Flash 4010, Germany), with tungsten electron source and an accelerating voltage of 15 kV. The iron and oxygen compositions of the AC-Fe(0) particles were identified through EDS elemental mapping.

XPS analysis of Ac-Fe(0) was performed with AXIS-NOVA (Kratos Inc., base pressure 8.8×10^{-9} Torr) at the Korea Basic Institute (Jeonju center), applying monochromatic Al Kα radiation beam at 1,486.6 eV. Wide scan analyses were performed with a pass energy of 160 eV, and narrow scan analyses with a pass energy of 20 eV, dwell time of 100 ms and energy step size of 0.05 eV. Spectra have been charge corrected to the main line of the carbon 1s spectrum (adventitious carbon) set to 284.8 eV.

The pH was measured by using Inolab 740 (WTW).

RESULTS AND DISCUSSION

1. Characterization of AC-Fe(0) Particles

The surface area of particles in a heterogeneous reaction is an important parameter that controls the ability of the particles to react with other reagents. BET surface area of the particles tested in this experiment shows a large deviation. Unsupported Fe(0) nanoparticles show a BET value of 8.1±0.09 m^2/g, and AC shows a BET value of 603.2±9.9 m^2/g as expected by its porous structure. The BET value of AC-Fe(0) is much larger than that of unsupported Fe(0), but much smaller than that of AC itself. AC-Fe(0) (1 : 1) has a value of 280.2±3.8 m^2/g and AC-Fe(0) (5 : 1) a value of 333.9± 4.8 m^2/g. The particles with a higher AC ratio showed a larger BET value than the particles with a lower AC ratio. The decrease in BET surface area of AC upon the deposition of nano Fe(0) implies that some of the pores of AC are most likely filled by Fe(0) nanoparticles during the synthesis of AC-Fe(0). In another report, the surface area of iron-on-silica particles also decreased significantly than that of silica itself, suggesting that some of the iron is deposited into the pores of the silica [17]. This kind of clogging by nanosized Fe(0) can possibly affect the mass transport into the iron inside the pores and out to the bulk media, resulting in the decline of nitrate reduction rate.

The iron content of each particles was measured by ICP-AES, and the calculated and measured iron contents of various AC-Fe(0) particles are shown in Table 1. The calculated content of iron of the particles differs from that of the measured content. The loss of iron precursor during the preparation of the supported iron can be a reason for the discrepancy. The partial oxidation of Fe(0) during synthesis can be another reason, as the formation of iron oxides adds

Table 1. Calculated and measured iron content of various AC-Fe(0) particles and Fe(0) nanoparticles

Particles	AC : Fe(0)	Calculated content of AC : Fe(0) (% of iron)	Measured content of iron (ICP-AES)
Nano Fe(0)	0 : 1	0 g : 0.5 g (100%)	90%
AC-Fe(0) (1 : 1)	1 : 1	0.5 g : 0.5 g (50%)	37.7%
AC-Fe(0) (5 : 1)	5 : 1	2.5 g : 0.5 g (16.6%)	13.9%

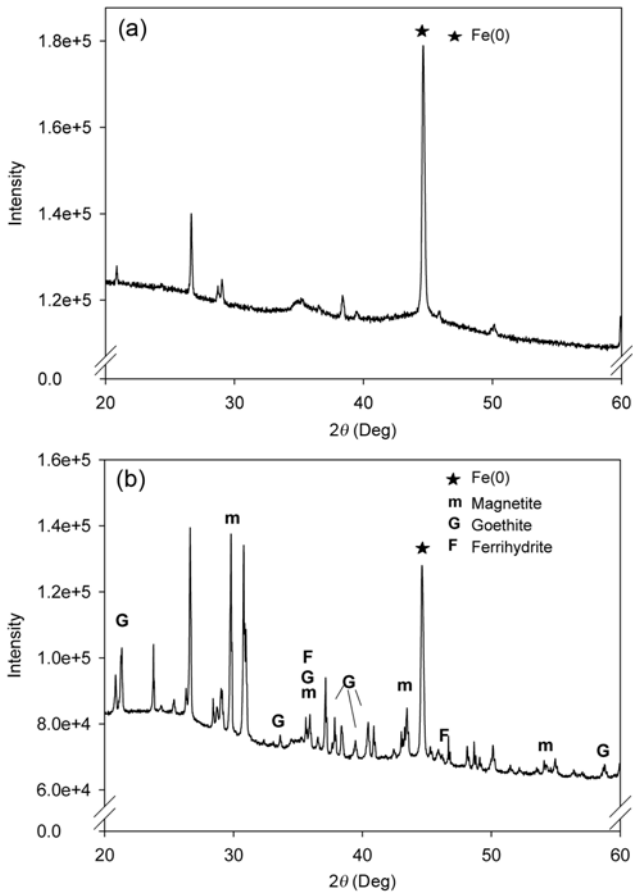

Fig. 1. X-ray powder diffraction patterns of AC-Fe(0) particles. (a) AC-Fe(0) (1 : 1). (b) AC-Fe(0) (5 : 1).

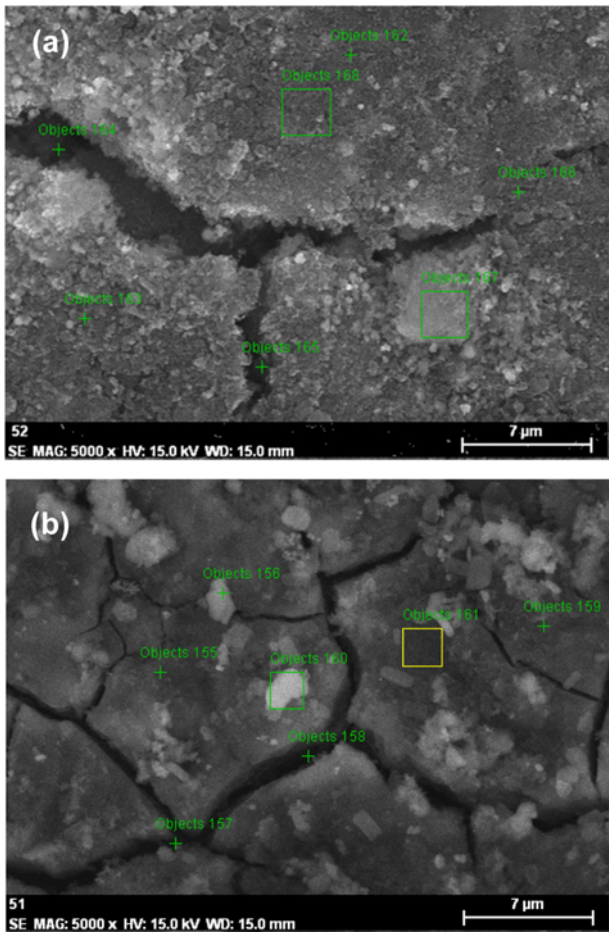

Fig. 2. SEM Images of AC-Fe(0) particles showing the EDS analysis areas and points and AC only. (a) AC-Fe(0) (1 : 1). (b) AC-Fe(0) (5 : 1).

a mass of oxygen to the total weight of particles and thus the relative percentage of iron will decrease. Also, the measured amount of iron of AC-Fe(0) particles is not the amount of zerovalent iron, as ICP-AES analysis does not give information on the local oxidation state of iron, but shows only the total amount of iron in a particle.

Nitrate reduction by Fe(0) is known to proceed via direct electron transfer on the Fe(0) surface as the main reaction path [18]; thus the amount of metallic iron in AC-Fe(0) particles is an important factor for the nitrate reduction. X-ray powder diffraction analyses (Fig. 1) provide useful information on the presence of iron oxide and metallic iron. Fig. 1(a) of AC-Fe(0) (1 : 1) particles shows mainly the signals corresponding to Fe(0) (star), indicating that most of the iron in this AC-Fe(0) particles exists in zerovalent state. Fig. 1(b) of AC-Fe(0) (5 : 1) particles shows the signal of Fe(0) and signals which can be assigned to diverse iron oxides, such as goethite, ferrihydrite and magnetite [19-21]. The formation of diverse iron(hydroxyl)oxides suggests that the oxidation process may proceed in a complex way.

In any case, Fig. 1(b) with higher content of AC reveals that a significant amount of iron in this particle exists in oxidized form, while Fig. 1(a) mainly shows the signals for Fe(0). This difference in the oxidation state of iron in the various AC-Fe(0) particles is reflected in the reactivity of particles for the nitrate reduction, which will be discussed in the next section.

Fig. 2(a) and Fig. 2(b) show the SEM images of the AC-Fe(0) particles. The squares and the points in SEM images (denoted by No.) are positions or areas for EDS analysis. Surface compositions corresponding to each No. in these AC-Fe(0) particles determined

Table 2. Unnormalized contents of Fe and O (in EDS analysis)

Particles	No. for EDS analysis in Fig. 2	Fe (%)	O (%)
AC-Fe(0) (5 : 1)	155	53.22	29.19
	156	41.12	39.63
	157	64.45	17.19
	158	82.82	5.80
	159	40.49	42.11
	160	28.12	44.89
	161	49.12	30.49
AC-Fe(0) (1 : 1)	162	65.05	6.00
	163	73.09	6.78
	164	95.51	0.61
	165	93.48	1.94
	166	71.10	4.15
	167	54.57	31.50
	168	52.27	16.04

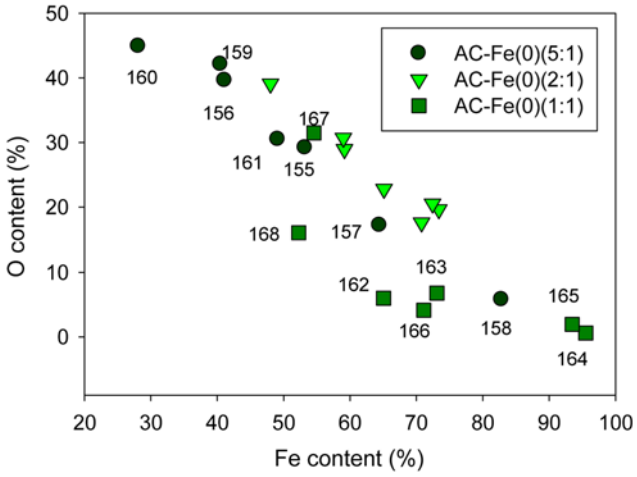

Fig. 3. Fe content vs. O content of various AC-Fe(0) particles.

by EDS analysis are given in Table 2, and the iron content of each No. was plotted against oxygen content to obtain the correlation line in Fig. 3. The black circles with numbers of 158-161 represent AC-Fe(0) (5 : 1) and the gray squares with numbers of 162-168 represent AC-Fe(0) (1 : 1). The upside-down triangles (numbers are omitted for clarity) represent AC-Fe(0) (2 : 1).

Fig. 3 reveals that iron content is adversely related to oxygen content. With decrease in iron content, oxygen content increases, and this correlation can be explained by the formation of iron oxides. As the zerovalent iron is oxidized to form iron oxides, the relative content of iron will decrease and the oxygen content will increase. Therefore, the data for AC-Fe(0) (5 : 1) particles (black circles) are found at the upper left side of the graph with higher oxygen content, and the data for AC-Fe(0) (2 : 1) (upside-down triangle) are located in the center of the graph, while the data for AC-Fe(0) (1 : 1) (gray square) are in the lower right part of the graph with the highest iron content among three different kinds of particles. Interestingly, the points 164 and 166 in the crack of Fig. 2(a) show over 90% of iron and less than 2% of oxygen, which indicates that the iron in this area exists mainly in zerovalent state. Further investigation is needed to give a clear explanation for that; however, it is obvious that the iron inside of the crack was protected from the oxidation. These phenomena are also observed in AC-Fe(0) (5 : 1) particles; the EDS data for position numbers of 157 and 158 in crack confirm higher iron and less oxygen content compared to other sites (155, 156, 159-161).

The carbon content from EDS data (detection of activated carbon) ranges from 0.2-1.5% for AC-Fe(0) (5 : 1), 0.2-0.7% for AC-Fe(0) (2 : 1) and 0.7-6.8% for AC-Fe(0) (1 : 1). Considering that the EDS analysis with 15 kV acceleration voltages normally covers the X-ray emission from elements within ca. 1 μm depth, this result indicates that the X-ray beam did not reach AC support and that the layer of iron coating on AC seems to be over a micrometer in thickness.

Further supplementary information on the oxidation state of iron on the surface of AC-Fe(0) can be obtained by X-ray photoelectron spectrometer. Fig. 4(a) shows the XPS wide-scan spectrum of Ac-Fe(0) (2 : 1). The spectrum contains the expected peaks from Fe 2p, O 1s and C 1s. XPS is a surface analysis technique analyzing

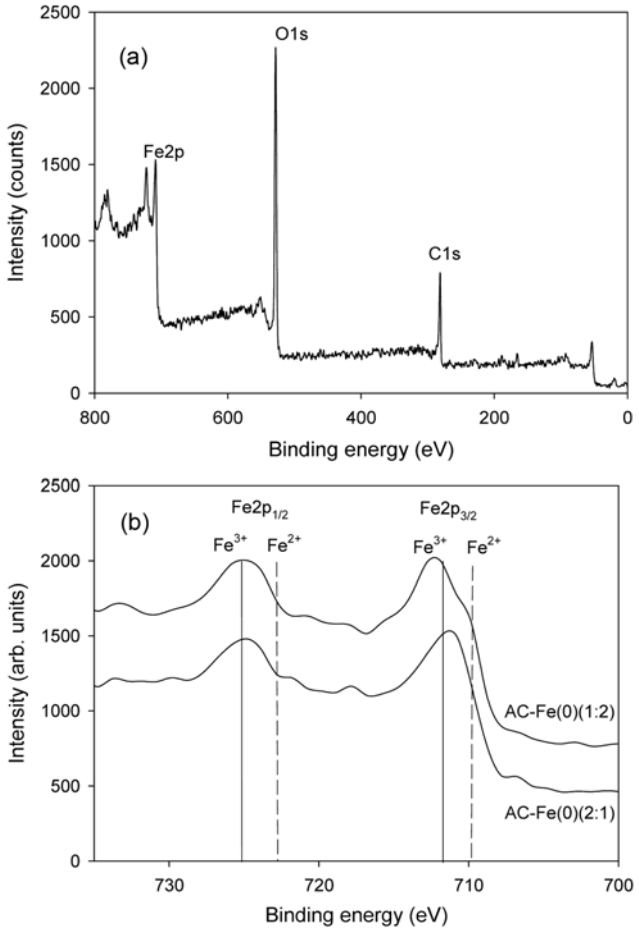

Fig. 4. XPS spectra. (a) Wide scan spectrum of AC-Fe(0) (2 : 1). (b) XPS spectrum of the Fe 2p region of AC-Fe(0) particles.

photoelectrons which originate from the outermost 1-10 nm of the sample. Nanosized zerovalent iron particle usually has a core-shell structure with ca. 5 nm iron oxide shell, and we assume that AC-Fe(0) particles have similar iron oxide shell [22-26]. Thus, it is not unexpected that iron in our sample was detected predominantly as Fe(III) from the oxide shell with minor Fe(II) present. Detailed XPS survey for Fe2p regions is shown in Fig. 4(b). Photoelectron peaks at ~710 and 722 eV (dashed line) correspond to the binding energies of $Fe2p_{1/2}$ and $Fe2p_{3/2}$ of Fe(II), respectively, and peaks at ~712 and 725 eV (solid line) correspond to the binding energies of $Fe2p_{1/2}$ and $Fe2p_{3/2}$ of Fe(III), respectively. Fe2p Peaks of various oxides are so closely spaced that differentiation between oxides that are formed on the surface of AC-Fe(0) particles is difficult [19]. XRD in Fig. 1(b) provides better information for that.

2. Influence of AC on the Nitrate Reduction of Fe(0)

The reactivity of the various AC-Fe(0) particles was compared with that of unsupported Fe(0) nanoparticles in Fig. 5. For all cases, the dosage of iron is 0.5 g and the amount of AC varies from 2.5 g for AC-Fe(0) (5 : 1), 1 g for AC-Fe(0) (2 : 1), 0.5 g for AC-Fe(0) (1 : 1), to 0.25 g for AC-Fe(0) (0.5 : 1). For the reaction of AC only, 2.5 g AC was used. The results show that immobilization of Fe(0) nanoparticles on AC significantly reduced the efficiency of nitrate reduction of Fe(0) in comparison to unsupported Fe(0) nanoparticles, while the degree of the reactivity decline varied with the amount

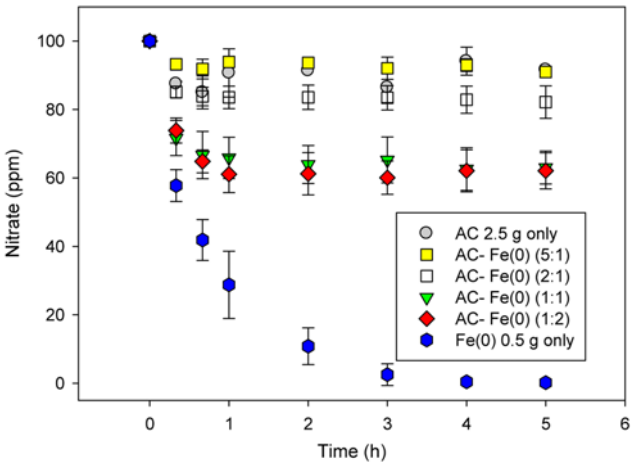

Fig. 5. Nitrate concentration - time curves of various AC-Fe(0) particles.

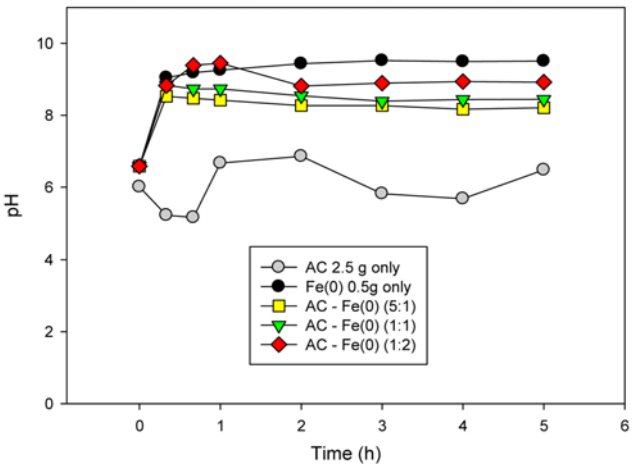

Fig. 6. pH - time plots of various AC-Fe(0) particles.

of AC support.

The square representing the reaction of AC-Fe(0) (5 : 1) particles shows a 10% removal of nitrate, and this amount of removal seems not to be the result of Fe(0) mediated reduction but mainly of the adsorption of nitrate on AC, which was verified from the result of AC only (circle) in Fig. 5. The reason why the AC-Fe(0) (5 : 1) has practically no nitrate reducing ability can be explained by the fact that much of the iron in this particle is already oxidized before it is applied to the reaction, and it is consistent with the results of XRD, SEM-EDS data for AC-Fe(0) (5 : 1) particles as described in the section of characterization of AC-Fe(0).

Upon reducing the amount of AC in AC-Fe(0) particles, the nitrate removal rate increased. AC-Fe(0) (2 : 1) shows a slightly better reactivity than AC-Fe(0) (5 : 1), AC-Fe(0) (1 : 1) and AC-Fe(0) (0.5 : 1) shows a similarly enhanced reactivity.

As can be predicted from the physicochemical characteristics of the AC-Fe(0) particles revealed by XRD, EDS and XPS analyses in the previous section, the reactivity decline of AC-Fe(0) nanoparticles seems in the first place to be due to the oxidation of iron on the surface of AC. Support materials provide a greater surface area where iron can be distributed during Fe(0) nanoparticles synthesis. At the same time, however, there is a greater chance for iron to contact air. The partial oxidation (mainly on the surface) of iron during the synthesis of iron nanoparticles and the storage is very difficult to avoid. In many literatures, the laboratory synthesized Fe(0) particles or commercially obtained Fe(0) particles show a core-shell structure, where the shell consists of iron oxide and it protects the inner core Fe(0) from further corrosion [22-26]. These protecting iron oxide coatings form sometimes due to uncontrolled oxidation during synthesis, or are intentionally formed [25,27].

The second possible reason for the decline of reactivity of AC-Fe(0) is the mass transport limitation caused by the thick layering of iron on the AC, at least 1 μm, as mentioned in the description of EDS analysis above. Piling up nanosized Fe(0) in a thick layer will reduce reactivity because it limits both the penetration of nitrate ions to reach the inner metallic iron, and escape of the product out of the thick layer into the bulk solution. Electron transfer may also be inhibited by these thick and non-conductive iron oxides film.

The third problem is related to the porous supporting materials. In the discussion of BET surface area of AC-Fe(0), it was mentioned that Fe(0) was deposited not only on the surface of AC but also inside of the pores of AC, thus the BET surface area of AC-Fe(0) is smaller than that of AC itself. Access to Fe(0) deposited on the inner surface of pore will be limited relative to the access to Fe(0) deposited on the outer surface of AC. In addition, the deposition of Fe(0) inside the pores of AC will reduce the pore volume, thereby limiting the mass transfer.

It has been reported in many studies that high pH of a solution has a significant negative impact on nitrate reduction by macro- and micro-sized Fe(0) particles, so that the appropriate pH for the nitrate reduction has been reported to be acidic [28-31]. However, in case of Fe(0) nanoparticles, the solution pH of the nitrate reduction increased rapidly to 9-10 within a few minutes after the beginning of the reaction and remained between 9-10 throughout the reaction [25]. Fig. 6 shows the pH profile during the reactions of various AC-Fe(0) with nitrate. The initial pH of the solutions with various AC-Fe(0) particles did not differ, so that the influence of the initial pH on the reactivity of various AC-Fe(0) could be excluded. As expected, the more reduction takes place, the higher the pH of the solution rises. For the unsupported Fe(0) nanoparticles, pH change is the greatest, while the reaction with AC-Fe(0) (5 : 1) (this particles shows the lowest reactivity for nitrate reduction) resulted in the least pH change.

Fig. 7 shows the results from the experiments where unsupported Fe(0) nanoparticles and AC were merely mixed in various ratios. Interestingly, AC is not a spectator but has a slightly negative influence on nitrate reduction. In the presence of AC, ca. 35% of the reactivity decline of Fe(0) nanoparticles was observed. The control experiment without Fe(0) reveals that 2.5 g of AC can adsorb ca. 9% of nitrate in a 100 ppm nitrate solution, while the adsorption by 0.5 g AC is negligible. It means that there are additional negative effects of the mixed AC besides adsorption. The hydrophobic character of AC might be one of the factors. Further investigation is needed to answer the question of the influence of AC in the mixture on the reactivity.

Ammonia was the major end product of the reduction process in all reactions performed in these experiments.

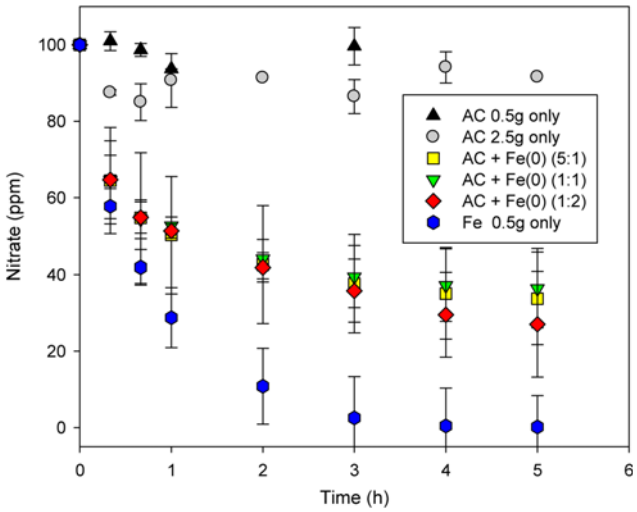

Fig. 7. Nitrate concentration - time curves of various AC+Fe(0) mixtures.

CONCLUSIONS

When using a support for nanoparticle synthesis, the negative aspects of the support should be considered as well as its positive aspects. The increased surface area and reactive sites, and the prevention of the agglomeration of nanoparticles and the resulting improvement in hydraulic conductivity due to a larger support can all be advantageous. However, the increased surface itself provides more place for Fe(0) to contact oxygen, which leads to corrosion as verified in this study with Fe(0) nanoparticles. It is especially true for Fe(0), unlike other metals of high positive reduction potential such as Pd, Pt, Ag, and Au etc. Furthermore, thick layering on the support hindered the mass transport of reagent components into the under-layered Fe(0), and internal Fe(0) deposited inside the pores of the AC has also a limited contact to the reagents, so that the significant amount of Fe(0) cannot actively participate in the reaction.

To take advantage of support, the ratio of AC to Fe(0) must be tuned so that the positive effects of using supported Fe(0) nanoparticles can overcome the negative effects.

ACKNOWLEDGEMENTS

This work was supported by the Korea Science & Engineering Foundation (R04-2004-000-10192-0).

REFERENCES

1. J. Kroschwitz and M. How-Grant, Eds. *Encyclopedia of chemical technology*, 4th Ed., J. Wiley & Sons, New York, **5**, 340 (1993).
2. J.-J. Li, X.-Y. Xu, Z. Jiang, Z.-P. Hao and C. Hu, *Environ. Sci. Technol.*, **39**, 1319 (2005).
3. M. Cho, E. Kim, K.-H. Lee and S. Ahn, *J. Environ. Sci.*, **17**, 711 (2008).
4. S. M. Ponder, J. G. Darab and T. E. Mallouk,. *Environ. Sci. Technol.*, **34**, 2564 (2000).
5. M. S. Ponder and T. E. Mallouk, U. S. Patent, 6,689, 485 B2 (2004).
6. J. G. Darab, A. B. Amonette, D. S. D. Burke and R. D. Orr, *Chem. Mater.*, **19**, 5703 (2007).
7. B.-W. Zhu, T.-T. Lim and J. Feng, *Chemosphere*, **65**, 1137 (2006).
8. L. Wu, M. Shamsuzzoha and S. M. C. Ritchie, *J. Nanopart. Res.*, **7**, 469 (2005).
9. United States Environmental Protection Agency, *National water quality inventory*, EPA 816-R-00-013; USEPA Office of Water: Washington, DC, August (2000).
10. H. H. Comly, *J. Am. Med. Assoc.*, **129**, 112 (1945).
11. P. J. Weyer, J. R.Cerhan, B. C. Kross, G. R. Hallberg, J. Kantamneni, G. Breuer, M. P. Jones, W. Zheng and C. Lynch, *Epidemiology*, **12**, 327 (2001).
12. United States Environmental Protection Agency. National Primary Drinking Water Regulations: Contaminant Specific Fact Sheets, Inorganic Chemicals, Technical Version; 811-F-95-002a-T; USEPA Office of Water, Washington, DC, (1995). Korean Minister of Environment, Drinking Water Quality Management 5-3 (2011).
13. The EU Water Framework Directive, European Commission Environment (2000).
14. N. P. Cheremisinoff and P. N. Cheremisinoff, *Carbon adsorption for pollution control,* PTR Prentice Hall, 19 (1993).
15. G. N. Glavee, K. J. Klabunde, C. M. Sorensen and G. C. Hadjipanayis, *Inorg. Chem.*, **34**, 28 (1995).
16. L. S. Clesceri, A. E. Greenberg and A. D. Eaton, *Standard methods for the examination of water and wastewater*, 20th Ed., 4-108, American Public Health Association, Washington, DC (1998).
17. S. M. Ponder, J. R. Ford, J. G. Darab and T. E. Mallouk, *Mater. Res. Soc. Sym. Proc.*, **556**, 1269 (1999).
18. L. J. Matheson and P. G. Tratnyek, *Environ. Sci. Technol.*, **28**, 2045 (1994).
19. R. M. Cornell and U. Schwertmann, *The iron oxides*, VCH, Weinheim (1996).
20. R. G. Ford, P. M. Bertsch and J. C. Seaman, *Clays Clay Miner.*, **45**, 769 (1997).
21. J. P. Gaviría, A. Bohé, A. Pasquevich and D. M. Pasquevich, *Physica B.*, **389**, 198 (2007).
22. E. E. Carpenter, S. Calvin, R. M. Stroud and V. G. Harris, *Chem. Mater.*, **15**, 3245 (2003).
23. Y. Liu, S. A. Majetich, R. D. Tilton, D. S. Sholl and G. V. Lowry, *Environ. Sci. Technol.*, **39**, 1338 (2005).
24. J. T. Nurmi, P. G. Tratnyek, V. Sarathy, D. R. Baer, J. E. Amonette, K. Pecher, C. Wang, J. C. Linehan, D. W. Matson, J. C. Penn and M. D. Driessen, *Environ. Sci. Technol.*, **39**, 1221 (2005).
25. K. Sohn, S. W. Kang, S. Ahn, M. Woo and S. K. Yang, *Environ. Sci. Technol.*, **40**, 5514 (2006).
26. W. Yan, A. A. Herzing, C. J. Kiely and W. X. Zhang, *J. Contam. Hydrol.*, **118**, 96 (2010).
27. L. Signorini, L. Pasquini, L. Savini, R. Carboni, F. Boscherini, E. Bonetti, A. Giglia, M. Pedio, N. Mahne and S. Nannarone, *Phys. Rev. B.*, **68**, 195423-1-195423-8 (2003).
28. M. J. Alowitz and M. M. Scherer, *Environ. Sci. Technol.*, **36**, 299 (2002).
29. C. P. Huang, H. W. Wang and P. C. Chiu, *Water Res.*, **32**, 2257 (1998).
30. Y. H. H uang and T. C. Zhang, *Water Res.*, **38**, 2631 (2004).
31. R. Miehr, M. M. Tratnyek, J. Z. Bandstra, M. M. Scherer, M. J. Alowitz and E. J. Bylaska, *Environ. Sci. Technol.*, **38**, 139 (2004).